Chirping the probe pulse in a coherent transients experiment

Sébastien J. Weber, Bertrand Girard, Béatrice Chatel

Chirping the probe pulse in a coherent transients experiment

Sébastien Weber,* Bertrand Girard, and Béatrice Chatel
CNRS-Université de Toulouse, UPS, Laboratoire Collisions, Agrégats Réactivité, IRSAMC, F-31062 Toulouse, France.
(Dated: December 18, 2009)

Coherent transients occur when a chirped pump pulse excites a two-level transition. They have been observed with an ultrashort probe pulse. Several studies have been dedicated to using various pump shapes. Here, we reverse the roles of the pump and the probe pulses. We show that, with a Fourier limited pump followed by a chirped probe pulse, similar effects can be observed. Finally, we consider the case of two pulses with opposite chirps.

PACS numbers: 42.65.Re; 32.80.Qk; 42.50.Md; 32.80.Rm

I. INTRODUCTION

For now more than twenty years, the pump-probe technique has been one of the most powerful experimental techniques to elucidate time-resolved dynamics using ultrashort lasers [1]. In a typical pump-probe experiment, the pump laser initiates the dynamics by exciting a combination of states. To measure the temporal evolution, a probe pulse is used to lead the system in a final state producing a signal which reveals the dynamics induced as a function of the pump-probe delay. Quite early some works have been done theoretically [2] as well as experimentally to emphasize the role of the probe. In particular it has been shown that a careful adjustment of the wavelength in wavepackets dynamics studies can give access to different pathway dynamics [3–5]. Also, changing the probe polarization allows one to observe different dynamics [6, 7]. In parallel, the advent of pulse shaping [8] has led to fascinating results in coherent control [9–11]. Many of these results have been obtained by manipulating the shape of the pump pulse [12–19]. Some results have been obtained by shaping the spectral phase of the probe in order to select the final state in Li_2 [20] or to exhibit vibrational dynamics in liquid phase [21]. Moreover, shaping the probe in phase and/or in polarization has been widely implemented in CARS experiments [22–24] to drastically reduce the non resonant background as well as to significantly enhance the resonant CARS signal. This leads also to a huge improvement of both the sensitivity and the spectral resolution. Interesting implementations have been performed including both coherent control and interferometry techniques to simplify the CARS set-up by single pulse phase control non linear Raman spectroscopy [24]. In the same way, people have used chirped probe to improve the spectral resolution [25] using their time-spectral homothetic transformation properties [26]. At the same time, we have studied in great details the interaction of a chirped pump with a two-levels systems [27]. The evolution of the population amplitude has been studied using an ultrashort probe. Contrary to CARS scheme, here we consider a two-photon transition with an intermediate state close to the one-photon transition. We propose to study the effect of a chirped probe in such scheme. A detailed comparative analysis is performed between the normal chirped pump - FT limited probe case and the reversed case with a FT limited pump pulse and a chirped probe pulse. Thus we emphasize that the probe plays a crucial role in the dynamic not only by fixing the analysis resolution but also by determining the temporal evolution behavior itself. Finally we demonstrate that for particular values of the probe and pump spectral phases, one can obtain a short dynamic even pump and probe are long. Moreover this can be a way to measure the spectral phase of the electric field.

II. PRINCIPLE

In this paper, we consider the pump-probe scheme within a three-level system. Each pulse is resonant with only one transition. The two transitions are excited successively by two pulses. These pulses can in general be shaped. However, only the cases where one of the pulses is Fourier transform limited and the other one is highly chirped is considered in this section. To understand these dynamics, we first recall the interaction of a chirped pulse with a two-level system (subsection II A). The evolution of the excited state probability amplitude is described during this interaction. Then, we examine the case of a chirped pump pulse followed by an ultrashort pulse (already addressed in previous studies [26–30]) (subsection II B) which probe the dynamic in the excited state. Finally the case of a chirped probe preceded by an ultrashort pump pulse, which triggers the dynamic, (subsection II C) is studied. We show that although the physical situations are different, these two cases lead to similar behaviors as a function of the delay.

*sebastien.weber@irsamc.ups-tlse.fr

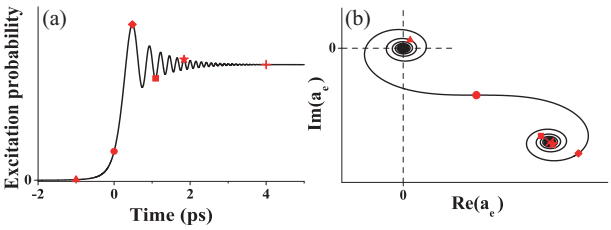

FIG. 1. Evolution of the upper state population under the excitation of a chirped pulse. (a): Probability exhibiting coherent transient; (b): Probability amplitude in the complex plane. The symbols correspond to different values of time τ: -1000fs (triangle), 0fs (circle), 480fs (diamond), 1090fs (square), 1840fs (star), 4000fs (cross) used for the simulations in fig. 4.

A. Interaction of a two-level system with a chirped pulse

In the temporal domain, the chirped pulse of duration T_C and angular frequency ω_C is written as :

$$E_C(t) = \mathcal{E}_0 \sqrt{\frac{T_0}{T_C}}\, e^{-t^2/T_C^2}\, e^{-i(\omega_C t - \alpha t^2)} \tag{1}$$

where T_C and α, are related to the chirp rate ϕ'' by :

$$T_C = T_0 \sqrt{1 + \left(\frac{2\phi''}{T_0^2}\right)^2}, \quad \alpha = \frac{2\phi''}{T_0^4 + (2\phi'')^2}. \tag{2}$$

T_0 is the duration of the corresponding Fourier limited pulse.

The lower and upper states are denoted $|g\rangle$ and $|e\rangle$ (named ground and excited state) respectively. First order perturbation theory gives the excited state probability amplitude during the resonant interaction ($\omega_C \simeq \omega_{eg}$) with the chirped pulse:

$$\begin{aligned} a_e(t) &= -\frac{\mu_{eg}}{2\hbar} \int_{-\infty}^{t} E_c(t)\, e^{i\omega_{eg}t'}\, dt' \\ &= -\frac{\mu_{eg}}{2\hbar} \int_{-\infty}^{t} \mathcal{E}_0 \sqrt{\frac{T_0}{T_p}}\, e^{-t'^2/T_C^2}\, e^{i(\omega_{eg}-\omega_C)t'}\, e^{-i\alpha t'^2} dt' \end{aligned} \tag{3}$$

The result of this interaction has been studied in detail [27] and is sketched in Fig. 1. The probability amplitude during this interaction follows a Cornu spiral (equivalent to the diffraction by a knife edge) in the complex plane (Fig. 1(b)). The excitation probability (Fig. 1(a)) presents a large increase when the instantaneous frequency goes through resonance. It is followed by oscillations which can be interpreted as beats between the atomic dipole excited at resonance and the instantaneous frequency which is shifting away from resonance. These oscillations are due to the quadratic phase which appears in the integral given by equation 4.

B. Chirped Pump pulse - Fourier Limited Probe pulse

In the scheme studied in previous works, this dynamics is observed in real time with a second ultrashort pulse as a probe. We consider therefore the simplest pump-probe scheme within a three-level system. These levels are named ground, excited and final state and denoted $|g\rangle$, $|e\rangle$ and $|f\rangle$ as shown in Fig. 2. The two sequential transitions $|g\rangle \rightarrow |e\rangle$ and $|e\rangle \rightarrow |f\rangle$ are respectively excited by a pump pulse $E_{pu}(t)$ of carrier angular frequency ω_{pu} close to resonance ($\delta_{pu} = \omega_{eg} - \omega_{pu}$, $|\delta_{pu}| \ll \omega_{eg}$), centered on $t = 0$ and by a probe pulse $E_{pr}(t)$ of carrier angular frequency ω_{pr} close to resonance ($\delta_{pr} = \omega_{fe} - \omega_{pr}$, $|\delta_{pr}| \ll \omega_{fe}$) and centered on $t = \tau$. The fluorescence arising from the $|f\rangle$ state can be recorded as a function of the pump-probe delay τ. The observed signal is proportional to the population $|a_f(\tau)|^2$ in the final state $|f\rangle$. The general expression of the probability amplitude $a_f(\tau)$ to find the system in the final state is given by second order perturbation theory :

$$\begin{aligned} a_f(\tau) = -\frac{\mu_{fe}\mu_{eg}}{4\hbar^2} \int_{-\infty}^{+\infty} dt' E_{pr}(t'-\tau) e^{i\omega_{fe}(t'-\tau)} \cdots \\ \times \int_{-\infty}^{t'} dt E_{pu}(t) e^{i\omega_{eg}t} \end{aligned} \tag{4}$$

In the first case, the pump pulse is chirped $E_{pu}(t) = E_C(t)$. The probe pulse is ultrashort and Fourier limited. This scheme is depicted in Fig. 2(a). The interaction takes place from the beginning of the chirped pulse until time τ when the ultrashort probe is applied. For a probe much shorter than the dynamics induced in the system, we can consider it as a Dirac $E_{pr}(t-\tau) \propto \delta(t-\tau)$ and simplify Eq. (4). We obtain an expression similar to the resonant interaction of a chirped pulse with a two-level system (Eq. (4)) except that τ is now the pump-probe delay instead of the real time of the chirped pulse. One gets :

$$a_f(\tau) \simeq -\frac{\mu_{fe}\mu_{eg}}{4\hbar^2} \int_{-\infty}^{\tau} dt E_{pu}(t) e^{i\omega_{eg}t} \tag{5}$$

The final state population $|a_f(\tau)|^2$ as a function of the pump-probe delay τ is therefore similar to the real-time temporal evolution of the level $|e\rangle$ in the two-level case, as displayed in Fig. 1 and already widely studied [27] and manipulated [18, 26, 28].

C. Fourier Limited Pump pulse - Chirped Probe pulse

We consider here the case of an ultrashort FT limited pump pulse followed by a chirped probe pulse. The ultra-

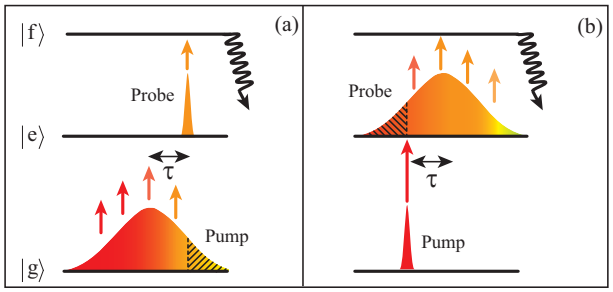

FIG. 2. Principle of the excitation scheme : (a) In the case of a chirped pump and a short probe, the probe "freezes" the interaction at time τ. (b) In the case of a short pump and a chirped probe, the pump triggers at time $-\tau$ (with respect to the chirped pulse) the interaction between the chirped pulse and the upper two levels.

short pump pulse can also be approximated by a Dirac so that

$$a_f(\tau) \simeq -\frac{\mu_{fe}\mu_{eg}}{4\hbar^2}\int_{-\infty}^{+\infty} dt' E_{pr}(t'-\tau)e^{i\omega_{fe}(t'-\tau)} \ldots \times \int_{-\infty}^{t'} dt\delta(t)e^{i\omega_{eg}t} \quad (6)$$

with,

$$\int_{-\infty}^{t'} dt\delta(t)e^{i\omega_{eg}t} = \begin{array}{ccc} 1 & : & t'>0 \\ 0 & : & t'<0 \end{array}$$

then,

$$a_f(\tau) \simeq -\frac{\mu_{fe}\mu_{eg}}{4\hbar^2}\int_{0}^{+\infty} dt' E_{pr}(t'-\tau)e^{i\omega_{fe}(t'-\tau)} \simeq -\frac{\mu_{fe}\mu_{eg}}{4\hbar^2}\int_{-\tau}^{+\infty} dt' E_{pr}(t')e^{i\omega_{fe}(t')} \quad (7)$$

which means that in this case the dynamics induced by the chirped pulse between the two upper levels is triggered by the pump (cf figure 2(b)). Although Eq. (7) is similar to the previous case (Eq. (5)), the interpretation of the observed oscillations is less straightforward. Indeed, the observed signal is not directly related to the dynamics of the upper level (here $|f\rangle$) excited by the chirped pulse. Modifying the value of τ changes only the starting time of the dynamics. The measured signal is the final result, at the end of these dynamics.

To better explain the difference between the delay τ and the real time t in this situation, Figure 3 presents a 2D plot of the $|f\rangle$ state population as a function of time t and delay τ. A horizontal cut corresponds to the real-time dynamics in the upper state. Several of such cuts (along the horizontal dashed lines in Fig. 3)correspond to the temporal evolution for a given pump-probe delay. They are displayed in the left hand side of Fig. 4. A vertical cut at a time longer than the chirped pulse duration corresponds to the final population as a function of the delay τ (see Fig. 3, right hand side). The same oscillations as with usual Coherent Transients are predicted. Indeed, Eq. (5) and (7) are completely similar if the pump and probe spectral phases are inverted.

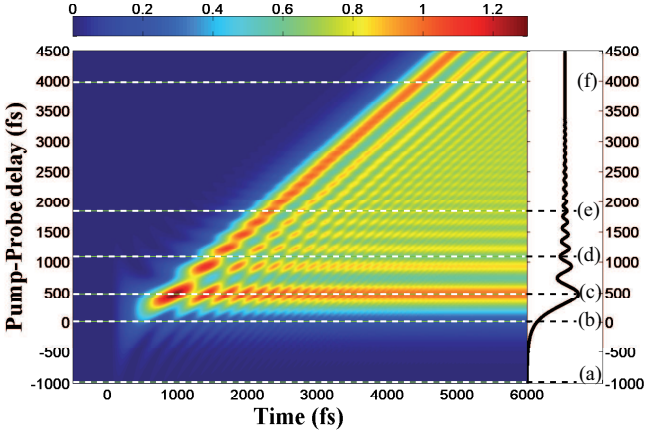

FIG. 3. 2D mapping of the final state population (normalized to the population at long time and delay) : the vertical axis is the delay between the pump and the probe, the horizontal axis is the time evolution. A vertical cut at 6 ps is plotted on the right side. It corresponds to the evolution of the asymptotic value of the final population. This is the one which is measured via the experiment. Several horizontal dashed lines are plotted. They correspond to the different cases presented on figure 4.

Another way to understand these predictions is to plot, in the complex plane, the temporal evolution of the probability amplitudes in the $|f\rangle$ state (right hand panels of Fig. 4) for various delays. For the largest delay $\tau = 4000$ fs (Fig. 4(f)), the pump pulse arrives long before the chirped pulse so that the whole dynamics can take place. One sees again the Cornu spirals, starting from the origin and finishing at the asymptotic value which corresponds to the measured quantity. On the left-hand panel, the population exhibits the same coherent transients as in the usual situation (see Fig. 1). At the opposite, for large negative values of τ, the probe arrives before the pump and the signal (left) is negligible. Moving now from large positive values to shorter delays ($\tau = 1840$ fs, 1090 fs and 480 fs for Fig. 4(e), 4(d) and 4(c) respectively), a progressively larger fraction of the leading part of the chirped pulse is inactive. Thus part of the beginning of the spiral is suppressed. In the complex plane, the curve starts always from the origin. Therefore the truncated spiral needs to be shifted. The new starting points are shown by red symbols on Fig. 1(b). The remaining curve is therefore shifted. The fi-

nal point is alternatively further, closer and further from the origin, corresponding to maxima and minima of the asymptotic values and therefore of the upper state population (left). One should notice that although having strong similarities with CT, these curves are not CT. In particular small oscillations are observed before the rising edge (see for instance Fig. 4(d)). This is a consequence of the truncated spiral. At $\tau = 0$, the pump pulse is at the maximum of the chirped pulse. Exactly half of the spiral is left. The final probability amplitude is half the one reached for largest values of τ and the population is one fourth. Finally, for negative delays, very weak oscillations are observed.

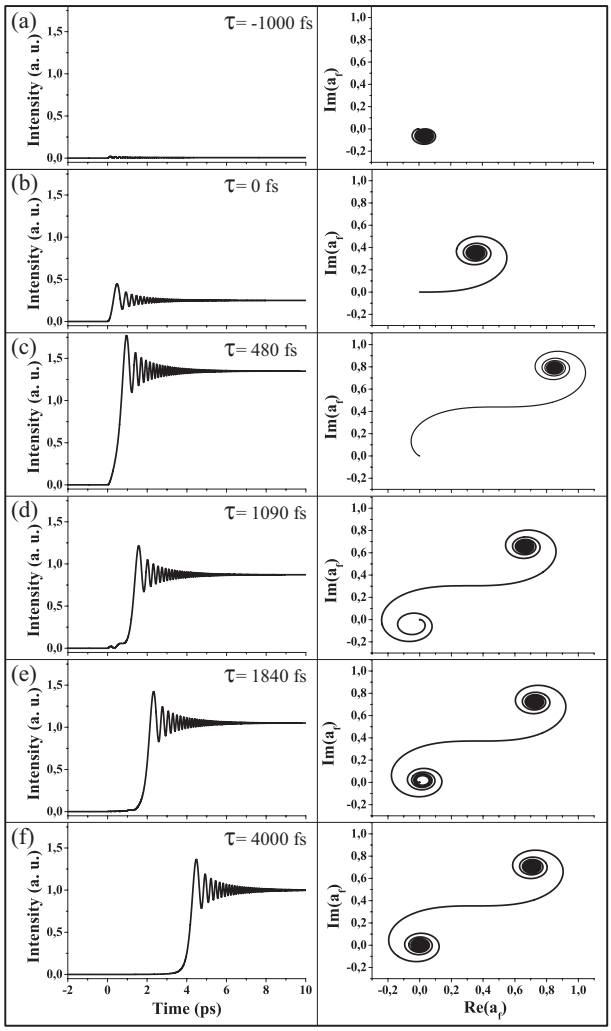

FIG. 4. Left: Temporal evolution of the final population during the probe pulse (normalized to the population at long time and delay); Right: Corresponding probability amplitude plotted in the complex plane. Pump-probe delays are −1000fs (a), 0fs (b), 480fs (c), 1090fs (d), 1840fs (e), 4000fs (f)

Another way to explain these behaviors is to notice that the population is simply the square of the distance between the starting and final point of the evolution of the probability amplitude. Therefore only the relative evolution is meaningful and it is not necessary to center the starting point of the truncated spiral at the origin. Each curve on Fig. 4 (left) is therefore obtained by plotting the square of the distance between an arbitrary origin on the spiral (corresponding to the value of the delay τ) and a point moving on the spiral. This explains more clearly why oscillations are obtained before the rising edge, when both starting and final points are within the same part of the spiral Fig. 4(d) (left).

When considering the asymptotic value (in other words, the observed pump-probe signal), it is also simpler to consider that the final point of the spiral is fixed. Thus, changing the delay τ (from $+\infty$ to $-\infty$) is simply equivalent to removing progressively larger parts of the spiral. One fully understands why the situation (for the pump-probe signal) is exactly symmetric to the first case when the pump is chirped.

III. EXPERIMENTAL RESULTS

To illustrate this point, an experiment has been performed in an atomic Rb vapor (figure 5). The Rb (5s - 5p ($P_{1/2}$)) transition (at 795 nm) is almost resonantly excited with an ultrashort pump pulse (The laser spectrum is centered around 808 nm with a FWHM of 24 nm).

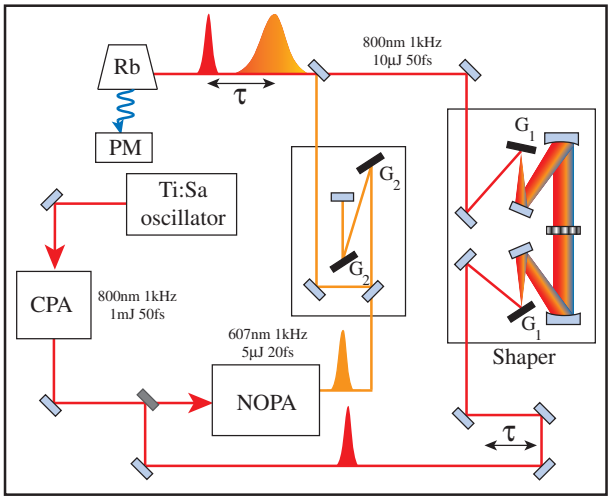

FIG. 5. Experimental set-up : G2: gratings with 600 grooves/mm G1:gratings with 2000 grooves/ mm; NOPA : Non colinear Optical Parametric Amplifier.

The transient excited state population is probed "in real time" on the (5p - (8s, 6d)) transitions with a pulse produced by a home-made NOPA (603 nm, 25 fs). This probe pulse is negatively chirped ($\phi''_{pr} = -1.4\,10^5$ fs^2) by a pair of gratings, recombined with the pump pulse and sent into a sealed rubidium cell with fused silica Brewster-window ends [18, 27, 28]. The pump can be shaped using a high resolution pulse shaper [31] formed by a double LC-SLM (640 pixels) placed in a Fourier plane of a highly dispersive 4f line. One takes care to block the red part

of the spectrum in order to avoid any two-photon transition (at 778 nm) and spin-orbit oscillations (at 780 nm) [32]. The pump-probe signal is detected by monitoring the fluorescence at 420 nm due to the radiative cascade $(ns, n'd) \rightarrow 6p \rightarrow 5s$. As expected, strong oscillations appear clearly on the black dots curve in Fig. 6 when the probe is chirped. These oscillations are similar to the coherent transients observed previously with the chirped pump [27]. The contrast is excellent and experimental data (black dots) fit well with theoretical data (gray solid line) obtained by analytical resolution of Eq. (4).

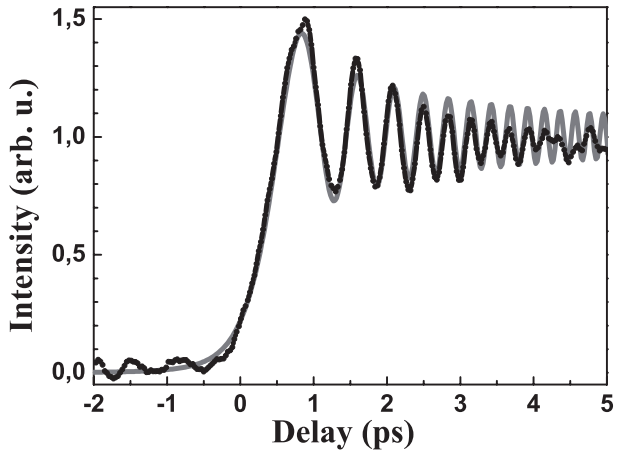

FIG. 6. Experimental Coherent Transients on Rb (5s-5p at 795 nm), for a chirp of $\phi''_{pr} = 1.4\,10^5$ fs^2 on the probe (black dots) and the corresponding simulation obtained by numerical resolution of the Schrodinger equation (solid line).

To demonstrate drastically the interplay of the pump and probe role, different amount of chirp are applied on the pump pulse using the shaper. Eq. 4 can be calculated exactly and leads to a rather complex expression in the general case of non-zero detunings (which is the case here) [33]:

$$a_f(\tau) \propto \frac{1}{\sqrt{\beta_{pu}\beta_{pr}}}\left[1 - \mathrm{erf}\left(-\frac{\gamma\sqrt{\beta_{\mathrm{pu}}+\beta_{\mathrm{pr}}}}{2\sqrt{\beta_{\mathrm{pu}}\beta_{\mathrm{pr}}}}\right)\right] \quad (8)$$

$$\gamma = \frac{i\left(\beta_{pu}\delta_{pr} - \beta_{pr}\delta_{pu}\right) - 2\beta_{pu}\beta_{pr}\tau}{\beta_{pu}+\beta_{pr}}$$

with $\beta_k = \frac{1}{T^2_{C,k}} + i\alpha_k$, δ_k $(k = pu, pr)$ is the detuning of the two pulses with respect to their transition frequencies and erf is the error function. The complex part of the argument of the erf function is responsible of the oscillations while the real part sets the rising time. Setting fixed the chirp of the probe and varying the one of the pump, the evolution of the final state could be drastically changed (see Fig. 7).

An interesting case is the one where chirp on pump and probe are opposite and fulfill $\phi''_k \gg T^2_{0,k}$. One gets the simplified expression for identical bandwidths ($T_{0,pu} = T_{0,pr} = T_0$) :

$$a_f(\tau) \propto T_0\, T_C\left[1 - \mathrm{erf}\left(-\frac{\tau}{\sqrt{2}\mathrm{T}_0} + \eta\right)\right] \quad (9)$$

$$\eta = -\frac{(\phi''_{pu}\delta_{pr} + \phi''_{pr}\delta_{pu})}{\sqrt{2}T_0} + i\frac{T_0}{2\sqrt{2}}(\delta_{pr} - \delta_{pu})$$

Two comments can be addressed:

- For zero detuning $\delta_k = 0$, the evolution of $a_f(\tau)$ is a simple step with a rising time equal to $\sqrt{2}T_0$. The oscillations are vanishing. The obtained dynamic is the same as with two Fourier Limited pulses. $\sqrt{2}T_0$ is their crosscorrelation duration.

- In the general case with detuning, η (Eq. 9) is a complex number. Its real part delays the step while its complex part gives a sharp peak around $\tau = 0$ well known as crosscorrelation peak [34] (see Fig. 7 (d)).

Experimental data are presented in Fig. 7 with $\phi''_{pr} = -1.4\,10^5$ fs^2 ($T_C \simeq 10$ ps) on the probe and $\phi''_{pu} = 0$ fs^2 (a), $\phi''_{pu} = 1.0\,10^5$ fs^2 (b), $\phi''_{pu} = 1.2\,10^5$ fs^2 (c), $\phi''_{pu} = 1.4\,10^5$ fs^2 (d) and $\phi''_{pu} = 1.5\,10^5$ fs^2 (e). Due to laser constraint, there is a large detuning on the pump. However one can see that the oscillations of the transients are vanishing when chirps on pump and probe become opposite (case (d) and (e)). As predicted by Eq. 9, the cancelation of the chirps leads to the shortest rising time of the pump probe signal, of the order of 60 fs (case (d)). For case (e), the evolution is a simple step with no peak and no oscillations despite the large detuning of the laser. This behavior can be explained, especially the absence of the sharp peak, by a fine balance between chirp and detuning in the complex time dependant part of γ (Eq. 8). Thus the best criterion for a chirp compensation is not the cancelation of the oscillations but the sharpness of the slope. The sensitivity of the coherent transients could thus be used as a fine adjustment of the pump chirp. This value is determined here with an accuracy of 10%, but this can certainly be improved.

This method could be used to determine the spectral phase of an unknown pulse. This approach will be particularly appropriate when one of the pulse is in a spectral range where it cannot be easily characterized. Further work is under study to see how the combination of complex spectral phases for both pump and probe pulses can be used as a useful tool for time resolved spectroscopies.

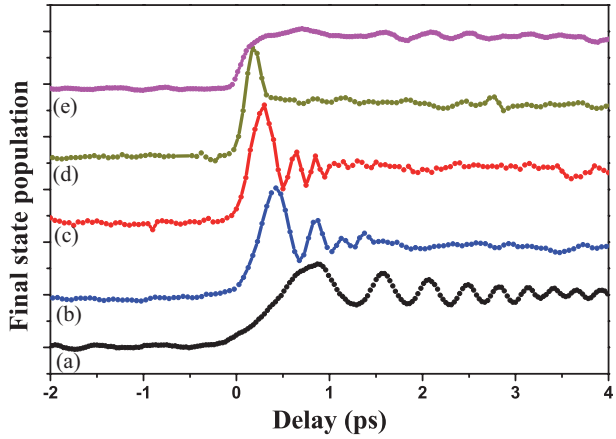

FIG. 7. Experimental Coherent Transients measured for a chirp of $\phi''_{pr} = -1.4\,10^5$ fs^2 on the probe and sequential chirp values for the pump (ϕ''_{pu}). The (a) black dot-solid curve correspond to transients obtained with a FL pump (see Fig. 6) plotted here for comparison. In blue, curve (b) $\phi''_{pu} = 1.0\,10^5$ fs^2 ; in red, curve (c) $\phi''_{pu} = 1.2\,10^5$ fs^2 ; in green, curve (d) $\phi''_{pu} = 1.4\,10^5$ fs^2 ; in purple, curve (e) $\phi''_{pu} = 1.5\,10^5$ fs^2. The increasing chirp of the pump gives less oscillations in the transients. For opposite chirps (curve d), the oscillations are completely removed (such as curve (e)) but the rising time obtained is here the shortest. It is equivalent to the FL cross-correlation duration. The sharp peak around $\tau = 0$ is due to the detuning of the central laser wavelength with respect to the resonance wavelength.

IV. CONCLUSION

In this paper we have demonstrated how the phase of the probe pulse could affect significantly the pump-probe signal, in an equivalent way as the phase of the pump. An illustrative experiment has been performed in rubidium vapor. Indeed, the spectral phases of the two pulses contribute equally. This was clearly demonstrated with two pulses of opposite chirp. A pump-probe signal with a very short rising time followed by a plateau has been obtained even with strongly chirped pump and probe pulses. This opens the route towards new pump-probe schemes where both pump and probe spectral phases can be shaped. It should be noted that this situation is opposite to the sum-frequency generation. Indeed, it was observed in this latter case [35, 36] that a long pulse with narrow bandwidth is generated. The presence of the resonant intermediate level creates the short transient.

We sincerely acknowledge Elsa Baynard for her technical help and Chris Meier and Sébastien Zamith for fruitful discussions.

[1] A. H. Zewail, *Femtochemistry: Ultrafast Dynamics of the Chemical Bond*, Vol. I and II (World Scientific, Singapore, 1994).
[2] H. Metiu and V. Engel, J. Chem. Phys. **93**, 5693 (1990).
[3] C. Nicole, M. A. Bouchene, C. Meier, S. Magnier, E. Schreiber, and B. Girard, J. Chem. Phys. **111**, 7857 (1999).
[4] H. Katsuki, H. Chiba, B. Girard, C. Meier, and K. Ohmori, Science **311**, 1589 (2006).
[5] H. Katsuki, H. Chiba, C. Meier, B. Girard, and K. Ohmori, Phys. Rev. Letters **102**, 103602 (2009).
[6] S. Zamith, M. A. Bouchene, E. Sokell, C. Nicole, V. Blanchet, and B. Girard, Eur. Phys. J. D **12**, 255 (2000).
[7] E. Sokell, S. Zamith, M. A. Bouchene, and B. Girard, J. Phys. B **33**, 2005 (2000).
[8] A. M. Weiner, Rev. Sci. Instr. **71**, 1929 (2000).
[9] A. Assion, T. Baumert, M. Bergt, T. Brixner, B. Kiefer, V. Seyfried, M. Strehle, and G. Gerber, Science **282**, 919 (1998).
[10] T. C. Weinacht, J. Ahn, and P. H. Bucksbaum, Phys. Rev. Lett. **80**, 5508 (1998).
[11] J. L. Herek, W. Wohlleben, R. J. Cogdell, D. Zeidler, and M. Motzkus, Nature **417**, 533 (2002).
[12] D. Meshulach and Y. Silberberg, Nature **396**, 239 (1998).
[13] N. Dudovich, B. Dayan, S. M. Gallagher Faeder, and Y. Silberberg, Phys. Rev. Lett. **86**, 47 (2001).
[14] P. Balling, D. J. Maas, and L. D. Noordam, Phys. Rev. A **50**, 4276 (1994).
[15] B. Chatel, J. Degert, and B. Girard, Phys. Rev. A **70**, 053414 (2004).
[16] R. Netz, A. Nazarkin, and R. Sauerbrey, Phys. Rev. Lett. **90**, 063001 (2003).
[17] M. Wollenhaupt, A. Prakelt, C. Sarpe-Tudoran, D. Liese, T. Bayer, and T. Baumert, Phys. Rev. A **73**, 063409 (2006).
[18] A. Monmayrant, B. Chatel, and B. Girard, Phys. Rev. Lett. **96**, 103002 (2006).
[19] K. Ohmori, Annual Review of Physical Chemistry **60**, 487 (2009).
[20] X. Dai and S. Leone, J. Chem. Phys. **127**, 014312 (2007).
[21] D. Polli, D. Brida, G. Lanzani, and G. Cerullo, CLEO/IQEC(2009).
[22] N. Dudovich, D. Oron, and Y. Silberberg, Nature **418**, 512 (2002).
[23] D. Oron, N. Dudovich, D. Yelin, and Y. Silberberg, Phys. Rev. Lett. **88**, 063004 (2002).
[24] Y. Silberberg, Annual Review of Physical Chemistry **60**, 277 (2009).
[25] K. P. Knutsen, J. C. Johnson, A. E. Miller, P. B. Petersen, and R. J. Saykally, Chemical Physics Letters **387**, 436 (2004), ISSN 0009-2614.
[26] W. Wohlleben, J. Degert, A. Monmayrant, B. Chatel, M. Motzkus, and B. Girard, Appl. Phys. B **79**, 435 (2004).
[27] S. Zamith, J. Degert, S. Stock, B. de Beauvoir,

V. Blanchet, M. A. Bouchene, and B. Girard, Phys. Rev. Lett. **87**, 033001 (2001).
[28] J. Degert, W. Wohlleben, B. Chatel, M. Motzkus, and B. Girard, Phys. Rev. Lett. **89**, 203003 (2002).
[29] A. Monmayrant, B. Chatel, and B. Girard, Opt. Lett. **31**, 410 (2006).
[30] A. Monmayrant, B. Chatel, and B. Girard, Opt. Commun. **264**, 256 (2006).
[31] A. Monmayrant and B. Chatel, Rev. Sci. Instr. **75**, 2668 (2004).
[32] B. Chatel, D. Bigourd, S. Weber, and B. Girard, J. Phys. B **41**, 074023 (2008).
[33] S. Zamith, *Dynamique femtoseconde dans des atomes et molécules: précession de spin et dynamique de photoélectrons, transitoires cohérents, dynamique des états excités de l'acétylène*, Thèse, Université Paul Sabatier (2001).
[34] I. V. Hertel and W. Radloff, Reports on Progress in Physics **69**, 1897 (2006).
[35] F. Raoult, A. C. L. Boscheron, D. Husson, C. Sauteret, A. Modena, V. Malka, F. Dorchies, and A. Migus, Opt. Lett. **23**, 1117 (1998).
[36] K. Osvay and I. N. Ross, Optics Communications **166**, 113 (1999).